Submission code: PRLJ5XDYRL

See this and other abstracts on our website: https://home.sbgf.org.br/Pages/resumos.php

Multichannel Blind Deconvolution assisted by Deep Learning

Andres Landeta (University of Campinas), Mauricio Sacchi (University of Alberta; Department of Physics), Amélia Novais (UNICAMP), Jörg Schleicher (University of Campinas)

Multichannel Blind Deconvolution assisted by Deep Learning

Please, do not insert author names in your submission PDF file.

Abstract Summary

Blind deconvolution, i.e., the simultaneous recovery of the seismic wavelet and reflectivity, is a fundamental challenge in seismic exploration. We tackle this ill-posed problem by means of a multichannel blind deconvolution approach assisted by deep learning, where machine learning provides an initial wavelet estimate. Specifically, we train a deep convolutional network to predict the wavelet from synthetic zero-offset seismic data. This predicted wavelet serves as the starting point for an minimization algorithm that alternatingly improves the reflectivity estimate and the wavelet. A well-initialized wavelet can significantly enhance the inversion process, leading to accurate wavelet and reflectivity recovery. However, the algorithm may converge to an incorrect solution if the initial estimate is too far from the true wavelet. We demonstrate that a machine-learning initial wavelet improves the chances for success. This underscores the critical role of machine learning in generating a reliable wavelet initialization, ultimately improving the robustness and stability of blind deconvolution.

Introduction

Wavelet processing is a critical component of reflection seismology. Accurate seismic wavelet recovery is crucial, as it directly links recorded seismic data to subsurface geology. Wavelet deconvolution enhances resolution by whitening the seismic spectrum, enabling traces to exhibit spectral characteristics that are more directly interpretable as reflectivity sequences.

Inspired by Canadas (2002) we propose a wavelet estimation method based on alternating minimization of a bilinear cost function. Given a set of seismic traces, each representing different reflectivity convolved with the same wavelet, the method alternates between estimating the wavelet using all traces (one-to-many optimization) and estimating the reflectivity for each trace given the wavelet (one-to-one optimization) (Bhuiyan and Sacchi, 2013). Remarkably, this approach converges reliably when initialized with a good wavelet approximation. This highlights the importance of a well-chosen starting point for successful wavelet recovery.

We hypothesize that a neural network trained on a sufficiently large and realistic dataset can provide a robust initial wavelet estimate. This estimate serves as the initialization for the alternating minimization framework, enabling recovery of both wavelet and reflectivity.

Alternating multichannel blind deconvolution

Building on the work of Canadas (2002), we formulate blind deconvolution as an alternating minimization problem. As usual, we estimate a single wavelet across all traces, while recovering individual sparse reflectivity series for each trace. Underlying is the well-established assumption that the wavelet remains stationary within a given analysis window, whereas reflectivity varies and exhibits

sparsity. The sparsity assumption allows for a parsimonious representation of seismic traces, modeling them as the convolution of a compact, short-duration wavelet with a sparse reflectivity sequence. Once the wavelet is estimated, any deconvolution technique can recover the reflectivity series, including classical methods that, while not explicitly enforcing sparsity, can still produce zero-phase, frequency-enhanced results.

We minimize the cost function

$$J = \sum_{j=1}^{n_x} \|\mathbf{W}\mathbf{r}_j - \mathbf{d}_j\|_2^2 + \lambda_w \|\mathbf{w} - \mathbf{w}_0\|_2^2 + \lambda_r \sum_{j=1}^{n_x} \|\mathbf{r}_j\|_1 \ , \tag{1}$$

where $\mathbf{d}_j$ (size $n_d \times 1$) represents the seismic trace at the j-th spatial position, and $\mathbf{r}_j$ (size $n_r \times 1$) corresponds to the reflectivity sequence. The wavelet $\mathbf{w}$, of length n_w, is embedded in the convolution matrix $\mathbf{W}$ (size $n_d \times n_r$) with $n_d = n_r + n_w - 1$.

The initial wavelet $\mathbf{w}_0$ ensures convergence to a good solution. Here, we estimate it with a neural network. We enforce the sparse-reflectivity assumption and introduce two trade-off parameters, λ_w and λ_r, to balance the regularization terms. The optimization proceeds by minimizing J alternately with respect to $\mathbf{r}_j$ and $\mathbf{w}$ while keeping the other fixed. Thus, our alternating minimization algorithm consists of two main steps:

1. Multichannel wavelet estimation using a Wiener filter.
2. Sparse reflectivity inversion by solving n_x ℓ_2-ℓ_1 problems via FISTA.

A network to estimate the initial wavelet

Conventionally, the initial wavelet $\mathbf{w}_0$ is a zero-phase wavelet with the amplitude spectrum of the data. We aim to improve $\mathbf{w}_0$ by means of a deep convolutional neural network, positioning it closer to the global minimum of the cost function (1), thus enhancing the convergence of our optimization problem. For this purpose, we adopt the Inception architecture (Szegedy et al., 2016) with a preprocessing stage and a final regression step to align the input and output data with the Inception network. The resulting network architecture is shown in Figure 1.

The training dataset consists of pairs of zero-offset gathers and wavelets. We divide the complete set of training pairs into 90% for training and 10% for validation.

Each seismic data set includes 1250 samples in time and 100 traces. To generate the zero-offset gathers, we convolve realistic geological reflectivity models obtained from the open-source project of Merrifield et al. (2022) with wavelets with 150 time samples. For this purpose, we create a library of Ricker wavelets, randomly varying the peak frequency between 5 Hz and 25 Hz and the phase rotation between $0°$ and $90°$.

To stabilize the process, we include an additional term to the traditional mean-square-error loss function by incorporating the differences of the Fourier amplitudes. This enhancement of the frequency-domain representation of the data led to improved wavelet estimates. The final cost function is then given by

$$E(\Theta) = \frac{1}{M}\sum_{i=1}^{M} \|\mathbf{w}_i - \hat{\mathbf{w}}_i(\Theta)\|_2^2 + \beta \frac{1}{M}\sum_{i=1}^{M} \| \, |\mathcal{F}[\mathbf{w}_i]| - |\mathcal{F}[\hat{\mathbf{w}}_i(\Theta)]| \, \|_2^2, \tag{2}$$

where M denotes the number of training examples, $\mathbf{w}$ and $\hat{\mathbf{w}}$ are the true and predicted wavelets, respectively, and β is the regularization parameter, set to 0.1. The term $|\mathcal{F}[\cdot]|$ denotes the amplitude of the Fourier transform. The learnable network weights and biases are encapsulated in the parameter Θ. Using the Adam optimizer, we train the neural network with the TensorFlow Keras library for 100 epochs, minimizing $E(\Theta)$ with a learning rate of 0.0001.

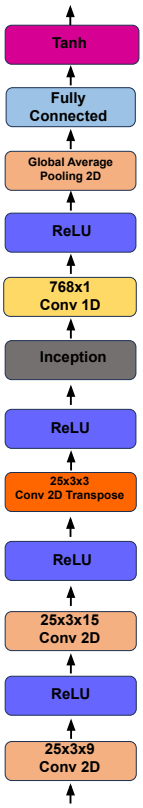

Figure 1: Network architecture.

Results

Synthetic noise-free data

To test our algorithm, we use a synthetic dataset with 147 data pairs, choosing different slices from a 3D velocity model, independently from the training data. To quantify the performance of our algorithm, we define the accuracy of the reconstruction by $Accuracy(dB) = 10\log\frac{\|\mathbf{x}\|_2^2}{\|\mathbf{x}-\bar{\mathbf{x}}\|_2^2}$, where $\mathbf{x}$ and $\bar{\mathbf{x}}$ denote the true and predicted signal, respectively. We conducted a series of experiments to systematically evaluate various regularization coefficients using a heuristic approach.

The selection criterion focused on the accuracy of reconstruction in order to balance the complexity and performance of the model. Finally, we set $\lambda_w = 0.01$ and $\lambda_r = 0.01$ and run 20 iterations to evaluate our algorithm.

Figure 2 shows the inversion results for five wavelets from the testing data and their amplitude spectra for comparison. The neural network demonstrates a strong ability to predict a good initial wavelet, which is then further improved by the multichannel inversion, both regarding the wavelets' shape and bandwidth.

To further study the dependence of the multichannel inversion on the initial wavelet and to evaluate the impact of the neural network in obtaining an improved initial wavelet, we conduct two experiments for synthetic test data with a $70°$ Ricker wavelet (Figure 3a). First, we solve the inverse problem using an initial wavelet predicted by the neural network (Figure 3b). The inversion result is depicted in Figure 3c.

In the second test, for comparison, we use a zero-phase Ricker wavelet with the true frequency content as the initial wavelet (Figure 3d). In this case, the inversion result (Figure 3e) deviates stonger from the true wavelet (Figure 3a), demonstrating that the inversion algorithm achieves the best results when a reasonable initial estimate constrains the optimization process. With the better starting point provided by the neural network, the inversion achieves a more accurate result.

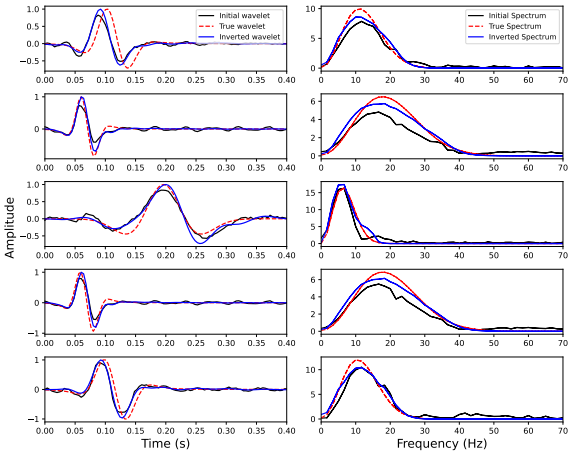

Figure 2: Comparison between the inverted result, the true wavelet, and the initial wavelet given by the neural network. Left: Time-domain traces. Right: Amplitude spectra.

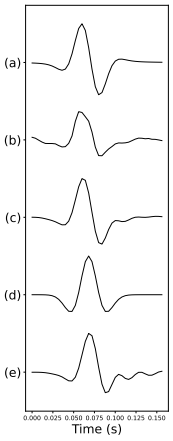

Figure 3: Comparison between wavelets: (a) true, (b) initial from neural network, (c) Inverted with (b), (d) initial zero-phase, (e) inverted with (d).

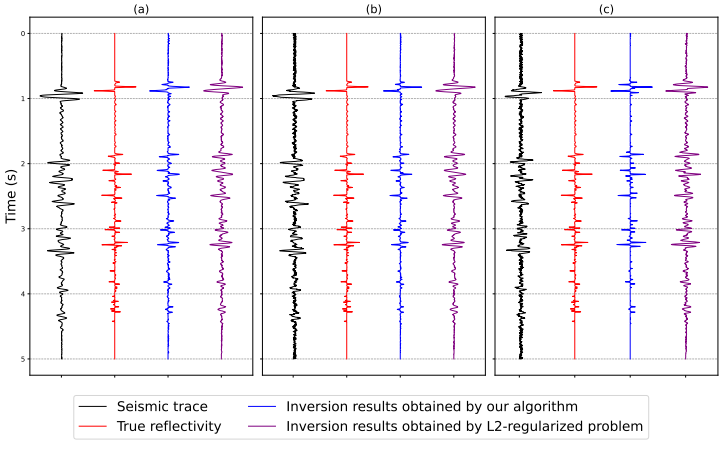

Figure 4: Comparison between our algorithm and L2-regularized problem: (a) inversion result for S/N of 100, (b) inversion result for S/N of 4, and (c) inversion result for S/N of 2.

Synthetic noisy data

To evaluate the effectiveness of our algorithm in this situation, we introduce white noise at three different levels to the seismic data, measuring the noise intensity using the signal-to-noise ratio (S/N) between the power of the clean signal and the power of the additive noise. The seismic data contain wavelets with in three different phase rotations ($0°$, $70°$ and $90°$) and 10 different peak frequencies. We use the same neural network as before without retraining to estimate the initial wavelets. Figure 4 compares the reflectivity inversion result for three seismic experiments with added noise. Panel (a) shows the results for a trace from the seismic section generated using a Ricker wavelet with a frequency of 13.91 Hz and zero phase, with an S/N of 100. Panel (b) shows the corresponding results with a Ricker wavelet of 18.5 Hz and 90° phase, with an S/N of 4. Finally, panel (c) presents the results for a Ricker wavelet of 17.89 Hz and 90° phase, with an S/N of only 2. We see that our algorithm produces good results under varying noise levels and wavelet characteristics, outperforming the L2-regularized procedure in all examples. Finally, Figure 5 summarizes the average accuracy and standard deviation of the wavelet inversion as a function of S/N. We observe good performance in noisy scenarios despite not retraining the neural network.

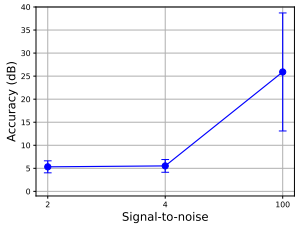

Figure 5: Mean and standard error of the wavelet inversion accuracy for the noisy data.

Conclusions

This work presents multichannel blind deconvolution assisted by deep learning. Our approach uses a deep convolutional neural network to estimate an initial wavelet, which is then used in a bilinear optimization problem to recover the seismic wavelet and the reflectivity model simultaneously.

The bilinear optimization depends strongly on the initial wavelet. The neural network, well trained with realistic models, provides versatility that not only accelerates the convergence of the optimization process but also enhances the stability of the solution. By providing an initial model close to the true wavelet, the neural network assists the optimization problem, helping the cost function to reach a minimum that optimizes the solution, thus reducing the risk of converging to suboptimal points.

Acknowledgments

A. Landeta acknowledges support from the Coordenação de Aperfeiçoamento de Pessoal de Nível Superior - Brasil (CAPES) - Finance Code 001. We are grateful to CNPq for supporting the INCT-GP.

References

Bhuiyan, M. M. I., and M. D. Sacchi, 2013, Two-stage blind deconvolution: GeoConvention 2013, Canadian Society of Exploration Geophysicists, 1–6.

Canadas, G., 2002, A mathematical framework for blind deconvolution inverse problems: SEG Technical Program Expanded Abstracts 2002, Society of Exploration Geophysicists, 2202–2205.

Merrifield, T. P., D. P. Griffith, S. A. Zamanian, S. Gesbert, S. Sen, J. D. L. T. Guzman, R. D. Potter, and H. Kuehl, 2022, Synthetic seismic data for training deep learning networks: Interpretation, **10**, no. 3, SE31–SE39.

Szegedy, C., V. Vanhoucke, S. Ioffe, J. Shlens, and Z. Wojna, 2016, Rethinking the inception architecture for computer vision: 2016 IEEE Conference on Computer Vision and Pattern Recognition (CVPR), IEEE, 2818–2826.